



Optimization of ultrasound-assisted extraction of *Imperata cylindrica* polysaccharides and evaluation of its anti-oxidant and amelioration of uric acid stimulated cell apoptosis

Wenchen Yu^{a,b,c,d}, Jiangfei Li^{b,c,d}, Yi Xiong^{a,b,c,d}, Junwen Wang^{b,c,d}, Jiaren Liu^c, Denis Baranenko^f, Yingchun Zhang^{b,c,d,e,*}, Weihong Lu^{b,c,d,e,*}

^a School of Chemistry and Chemical Engineering, Harbin Institute of Technology, Harbin, China

^b National and Local Joint Engineering Laboratory for Synthesis, Harbin Institute of Technology, Harbin, China

^c School of Medicine and Health, Harbin Institute of Technology, Harbin, China

^d Chongqing Research Institute, Harbin Institute of Technology, Chongqing, China

^e Zhengzhou Research Institute, Harbin Institute of Technology, Zhengzhou, China

^f School of Life Sciences, Faculty of Ecotechnologies, ITMO University, St. Petersburg. 197101, Russia

ARTICLE INFO

Keywords:

Imperata cylindrica

Ultrasonic-assisted extraction

Polysaccharide

ABSTRACT

An efficient, cost-effective and environmentally friendly ultrasound-assisted hot water method for *Imperata cylindrica* polysaccharide (ICPs) extraction was developed. According to the response surface results, the optimal ultrasonic time was 85 min, ultrasonic power was 192.75 W, temperature was 90.74 °C, liquid–solid ratio was 26.1, and polysaccharide yield was 28.50 %. The polysaccharide mainly consisted of arabinose (Ara), galactose (Gal), and glucose (Glc), with a molecular weight of 62.3 kDa. Ultrasound-assisted extraction of *Imperata cylindrica* polysaccharide (UICP) exhibited stronger anti-oxidant activity and ability to ameliorate cellular damage due to uric acid stimulation compared with traditional hot water extraction of *Imperata cylindrica* polysaccharide (ICPC-b). It also exhibited higher thermal stability, indicating its potential value for applications in the food industry.

1. Introduction

Plant polysaccharides, as highly polar macromolecules, possess the characteristic of being soluble in water but insoluble in ethanol. Therefore, they are generally extracted using the water extraction method [1]. This method is advantageous due to its simple principles and ease of operation. However, it requires high temperature and an extended extraction time [2]. In the rapid development of food industry, the traditional extraction methods of plant polysaccharides cannot meet the market demand. With the advancement of extraction technologies, ultrasonic technology has gradually gained widespread recognition and use in the extraction of plant polysaccharides [3]. Compared with traditional extraction methods such as organic solvent extraction, soxhlet extraction, and supercritical fluid extraction, ultrasonic extraction technology has the advantages of low energy consumption, low cost, short time, and high efficiency [4]. When ultrasound acts on a medium, it generates intense acoustic vibrations transmitted to the

medium, creating various effects while promoting heat and mass transfer [5]. Compared with traditional extraction methods, ultrasonic extraction has the advantage of low temperature, making it easier to obtain certain active components with thermal instability in natural materials [6]. Additionally, ultrasonic extraction technology has a wide range of extractable substances, a variety of solvent options, and weak dependence on the properties of natural materials and solvents [7]. Therefore, ultrasonic extraction technology has become a hot topic in the field of natural product extraction. Ultrasonic waves generate cavitation, mechanical, and thermal effects by breaking ultra bubbles, promoting the release of polysaccharides [8,9]. Hu [10] used ultrasound-assisted extraction to extract Ginkgo biloba seed polysaccharides and found that the polysaccharide yield with ultrasound-assisted extraction was 2.34 times that of hot water extraction. As mentioned above, ultrasound-assisted extraction is a method that can increase the yield of polysaccharides.

Imperata cylindrica, a traditional medicinal and edible plant in China,

* Corresponding authors at: National and Local Joint Engineering Laboratory for Synthesis, Harbin Institute of Technology, Harbin, China.

E-mail addresses: zhangyingchun@hit.edu.cn (Y. Zhang), lwh@hit.edu.cn (W. Lu).

contains chemical components such as triterpenoids, organic acids, etc. [11,12]. It exhibits various effects, including anti-oxidant [13], anti-inflammatory [14], anti-fibrotic [15], and cardiovascular protection [16]. In our previous study, we obtained crude *Imperata cylindrica* polysaccharide (ICPs) through traditional hot water extraction, and further obtained ICPC-b through alcohol precipitation and DEAE-52 purification [17]. The yield of ICPC-b was 17.50 %. We hypothesized that compared to traditional extraction methods, ultrasound-assisted could enhance the extraction and yield of ICPs. Therefore, a comparison between ultrasound-assisted and hot water extraction was conducted through analyses of molecular weight, monosaccharide composition, functional group changes, morphology, thermal properties, anti-oxidant activity, and the amelioration of uric acid-induced cell apoptosis.

2. Materials and methods

2.1. Materials and reagents

1,1-diphenyl-2-picrylhydrazyl (DPPH) was purchased from Nanjing Jiancheng Bioengineering Institute (Nanjing, China), and other reagents were obtained from Biyun Tian Biotechnology Co., Ltd (Shanghai, China).

2.2. Single factor experiments and optimized experimental design

The liquid–solid ratio, ultrasonic power, temperature, and time were investigated. The experimental conditions for ultrasound power encompassed 120 W, 160 W, 200 W, 240 W, and 280 W, while ultrasound time was varied at 40 min, 60 min, 80 min, 100 min, and 120 min. The temperature range was 60 °C, 70 °C, 80 °C, 90 °C, and 100 °C, the liquid–solid ratio set at 15 mL/g, 20 mL/g, 25 mL/g, 30 mL/g, and 35 mL/g. Employing Response Surface Methodology (RSM) and Box-Behnken design (BBD) [18], we optimized the extraction parameters by identifying the factors influencing the process.

2.3. Polysaccharide purification and molecular weight

The crude polysaccharides were concentrated and precipitated with 80 % ethanol. Further purification of ICPs was performed using DEAE-52 columns with varying concentrations of sodium chloride (0, 0.05, 0.1, 0.2 mol/L) and Sephadex G-100. High-Performance Gel Permeation Chromatography (Agilent, USA) was used to determine the molecular weight [19]. Chromatographic conditions: Agilent 1100 system equipped with TSK- GEL G3000-PWXL column (7.8 × 300 mm) and Agilent G1362A differential detector; Mobile phase: ultrapure water; Injection volume: 10 µL; Flow rate: 1.0 mL/min; Column temperature: 28 °C.

2.4. Monosaccharide composition detection

10 mg of ICPs was hydrolyzed with TFA (0.1 mol/L). Then it was reduced with sodium borohydride and treated with monosaccharide derivatization, and prepared with chloroform into 1 mg/mL solution. Then Agilent 1260 high performance liquid chromatography was used for detection [20]. The analysis used Agilent 1260 HPLC, Zorbax Eclipse Plus-C18 Chromatographic column. The specific detection conditions: the injection volume was 5 µL, the column temperature is 30 °C, the flow rate is 0.6 mL/min, and the mobile phase is A 0.025 mol/L potassium dihydrogen phosphate buffer: B acetonitrile = 83:17.

2.5. Determination of polysaccharide content

The total polysaccharide content in *Imperata cylindrica* was determined using the phenol–sulfuric acid method with a glucose standard curve. The procedure was repeated three times. Extraction yield of polysaccharide was calculated according to formula: $Yield (\%) =$

$$[(C \times V \times d)] \times 100$$

where C-content of total carbohydrates (mg/mL), V-original volume of filtrate (mL), d-dilution ratio, and m-weight of powders (g).

2.6. Characteristics of purified polysaccharides

2.6.1. Fourier transform infrared spectroscopy (FT-IR)

2 mg ICPs and 200 mg of potassium bromide (KBr) powder separately placed them in a pellet mold. Used a pellet press to create pellets. Used potassium bromide as a control to subtract the background. Scanned the infrared spectrum in the range of 400–4000 cm^{-1} on the Fourier transform infrared (FT-IR) spectrometer (Thermo Fisher Scientific) [21].

2.6.2. Congo red assay

ICPs was prepared into 1 mg/mL solution with distilled water and mixed with an equal volume of Congo red (100 µM). Scanning was done using an ultraviolet spectrophotometer with a wavelength range of 200 to 600 nm. Measure the maximum absorption wavelength at different concentrations.

2.6.3. SEM analysis

Used a scanning electron microscope (SEM, Thermo Fisher Scientific) to observe the solid-state appearance of ICPs. Placed the dried samples on a sample holder using double-sided tape, and sprayed gold powder onto the wafer using a sputter coater. Finally, observed the samples under the scanning electron microscope.

2.6.4. AFM analysis

Firstly, prepared a 1 mg/mL stock solution of ICPs, and stirred magnetically at 50 °C to reduce the aggregation of polysaccharides. Then, sequentially diluted the stock solution to 100 µg/mL and 10 µg/mL, repeated the magnetic stirring process, filtered to obtain the test solution, and took an appropriate amount for air-drying on mica sheets. The atomic force microscope (AFM) measurement conditions were as follows: used an un-dripped mica sheet as the scanning substrate, used a Si3N4 probe, scanned the microscopic morphology of ICPs, and finally obtained AFM images (scanning range: 1–10 µm, scanning frequency: 1.00 Hz) [17].

2.6.5. Thermal stability analysis

Determination of thermal stability of ICPs using thermogravimetric analysis (TG) and differential scanning calorimetry (DSC) [22]. 5 mg ICPs sample was placed in a platinum crucible and heated from 25 °C to 800 °C at 10 °C/min in a nitrogen atmosphere with a flow rate of 50 mL/min.

2.7. Anti-oxidant analysis

DPPH free radical scavenging activity was slightly modified based on the methods in the literature [23]. 1 mL of diluted extract was mixed with 2 mL of DPPH solution (0.2 mM) in a vortex, and the absorbance was obtained at 517 nm.

ABTS free radical scavenging activity was slightly modified according to the methods in the literature [24]. Mixed 10 mL ABTS (2 mM) with 100 µL potassium persulfate (70 mM) and stored at room temperature for 16 h away from light. The 100 µL diluted extract was mixed with 1 mL ABTS solution to, and the absorbance was obtained at 734 nm.

Detection of hydroxyl scavenging ability [25]. Added 1 mL FeSO_4 (9 mmol/L), 1 mL salicylic acid solution (9 mmol/L), 1 mL ICPs solution with different concentrations. Absorbance was measured at 510 nm.

The measurement of total reducing power was slightly modified according to the methods reported in the literature [26]. Added 0.5 mL 1 % potassium ferricyanide to 1 mL polysaccharide solution, 0.2 mol/L phosphate buffer of 0.2 mL pH6.6, and add 1 mL 10 % trichloroacetic acid, 10 µL 1 % FeCl_3 and 150 µL distilled water, and the absorbance was

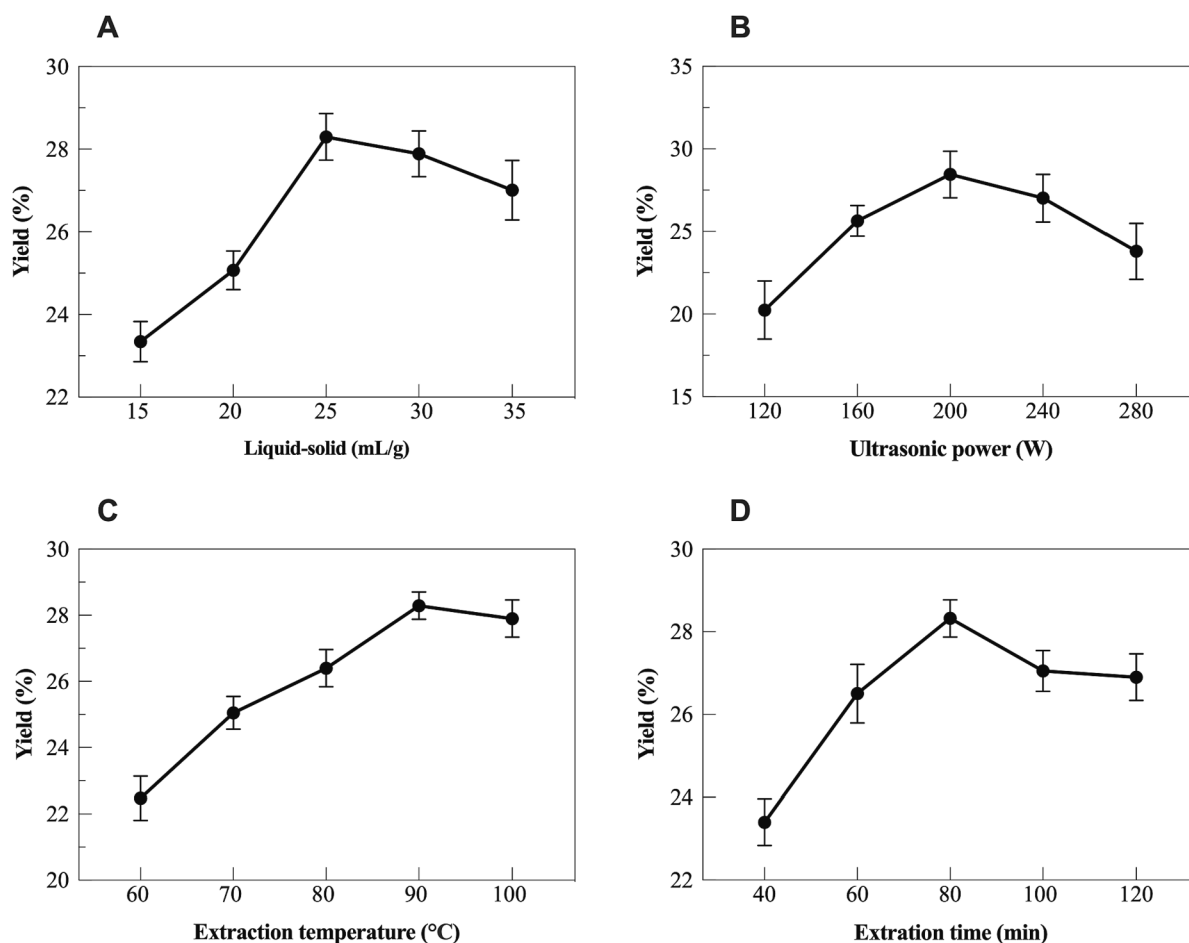


Fig. 1. The yield and recovery of ICPs extracted from different single factor experiments. A, extraction power; B, extraction time; C, extraction temperature; D, solid-liquid ratio.

measured at 700 nm.

2.8. Cell CCK8 assay

HK-2 (human renal cortex proximal convoluted tubule epithelial cells) were purchased from Institute of Cell Biology, Chinese Academy of Sciences. The HK-2 cells were seeded in 6-well plate (4×10^5 cells). After 24 h, the cells were replaced according to the grouping containing ICPs. Added uric acid and cultured in the incubator for 24 h. Added CCK-8 10 μ L and continue to incubate. Detected the cell activity by measuring the absorbance value of each well at 450 nm.

2.9. Cell apoptosis assay

HK-2 cells were washed once with PBS, trypsinized, and centrifuged. Annexin V and propidium iodide solution were added, and the mixture was shaken evenly. The cells were transferred to a flow tube for light-avoiding constant temperature incubation. After 30 min, apoptosis of the cells was detected using flow cytometry.

2.10. ROS detection

The serum-free medium containing 10 μ mol/L DCFH-DA was added. After incubation in a cell culture incubator for 30 min, centrifuged, and washed twice more. 200 μ L of PBS was added to suspend the cells. The suspended cells were transferred to flow tubes and subjected to flow cytometry to measure the cellular ROS levels.

2.11. Data analysis

All the displayed experimental data represented or counted the results of at least 3 independent experiments. Data analysis was performed using GraphPad Prism 9.0 software, and significance analysis was performed by Dunnett test.

3. Results and discussion

3.1. Single-factor extracting experiments of ICPs

We investigated the influence of parameters such as ultrasonic power, time, temperature, and liquid-solid ratio. As showed in the Fig. 1A, the polysaccharide yield increased more rapidly with an increase in the liquid-solid ratio. This can be explained by the increased solvent proportion caused a higher osmotic pressure, accelerating the outflow of substances from cells. The increase in solvent volume resulted in a larger ultrasound action area, leading to higher ultrasound efficiency [18]. Beyond 25 mL/g, the excessively high liquid-solid ratio led to a reduction in intermolecular interactions, causing a substantial decrease in the ultrasound penetration rate.

As the ultrasound power increased from 160 W to 200 W, there was a significant rise in the yield of ICPs, followed by a gradual decline (Fig. 1B). The intensified cavitation effects, thermal effects, and mechanical effects with the rise in ultrasound power contributed to the enhanced yield of ICPs [27]. However, excessive ultrasound power might lead to the degradation of polysaccharides in the solvent due to the impact of ultrasound.

Table 1
Experimental design and the results.

Run	Factor A Ratio (mL/ g)	Factor B Temperature (°C)	Factor C Power (W)	Factor D Time (min)	Yield (%)
1	30	100	200	80	26.85
2	20	90	240	80	24.07
3	20	90	200	60	24.34
4	30	80	200	80	25.09
5	25	90	200	80	28.46
6	25	80	200	60	24.70
7	30	90	200	100	26.95
8	20	80	200	80	24.25
9	25	90	240	100	25.35
10	25	100	200	100	27.23
11	30	90	200	60	25.10
12	30	90	160	80	26.74
13	25	90	240	60	24.60
14	25	90	200	80	28.35
15	25	90	160	60	25.62
16	25	90	200	80	28.13
17	20	90	200	100	24.98
18	25	80	240	80	24.53
19	25	80	200	100	25.66
20	25	90	200	80	27.95
21	25	90	200	80	28.18
22	20	100	200	80	24.82
23	25	100	200	60	25.78
24	30	90	240	80	25.06
25	25	100	160	80	27.05
26	25	80	160	80	25.50
27	20	90	160	80	24.74
28	25	90	160	100	27.11
29	25	100	240	80	25.33

The extraction yield of ICPs significantly increased from 22.47 % at 60 °C to 28.29 % at 90 °C, while the yield decreased after exceeding 90 °C (Fig. 1C). This may be because at higher temperatures, and surface tension decreases, leading to a lower intensity threshold for cavitation required by ultrasound, aiding the extraction process [28]. However, further increasing the temperature beyond 90 °C, the thermal effect can cause the degradation of polysaccharide structures, offsetting the increased mass transfer rate due to higher temperature [29].

The extraction yield of ICPs demonstrated an upward trend with the prolonged extraction time (Fig. 1D). Additionally, with prolonged ultrasound time, the continuous cavitation and microbubble implosion intensified the rupture of cell walls in plant materials, reducing the restriction of cell structure on the mass transfer process [30]. The decrease

in ICPs extraction yield may be attributed to prolonged ultrasound treatment time, resulting in transient high temperatures and released free radicals causing the degradation of polysaccharide substances [31].

3.2. Response surface optimization for ICPs extraction

Box-Behnken design (BBD) and the experimental values extracted by ICPs were showed in Table 1. The four factors mentioned above were used as the independent variables. The regression equations of polysaccharide on solid–liquid ratio (A), temperature (B), ultrasound power (C) time (D) were obtained as follows: $Y = 28.21 + 0.7158A + 0.6108B - 0.6517C + 0.5950D + 0.2975AB - 0.2525AC + 0.3025AD - 0.1875BC + 0.1225BD + 0.1850CD - 1.71A^2 - 1.24B^2 - 1.37C^2 - 0.16D^2$.

The surface experiment was designed based on single-factor experiments. According to Table 2., A, B, C, D, A², B², C², and D² were significantly affecting the yield of ICPs ($P < 0.01$); $R^2 = 0.9959$, $R^2_{adj} = 0.9918$, indicating that the model fits well and can more effectively analyze. The Adeq precision of the regression equation was 46.46, significantly larger than 4, indicating an ample signal response to the model. In summary, the proposed model demonstrates the ability to accurately and reliably predict ICPs under various conditions.

Fig. 2 illustrated the interaction between any two variables and their impact on the yield of ICPs. The yield of ICPs initially increased with the rise of factors A–D, followed by a decrease with the continuous increase of these factors. This trend aligns with the outcomes observed in the single-factor experiments. Steeper surface plots suggest more pronounced interaction effects [32].

The optimum process conditions were as follow: liquid–solid ratio 1:26.10 mL/g, ultrasonic power 192.75 W, extraction temperature 90.74 °C, and extraction time 88.84 min, under which the predicted polysaccharide yield was 28.50 %. A verification experiment was conducted using the optimal conditions as per the model. For the practical test, the average yield of polysaccharides was 28.22 % for three times under the conditions of liquid–solid ratio of 26 mL/g, ultrasonic power of 190 W, temperature of 91 °C, and time of 89 min. It indicated that the model optimization results are reliable. The yield of ICPC-b was 17.50 %, and it was significantly improved by ultrasonic-assisted extraction. Our research focused on the ultrasonic-assisted extraction method for polysaccharides. However, there are other methods to increase polysaccharide yield, such as the ultrasound-assisted hydrogen peroxide–ascorbic acid method [33], ultrasound-assisted enzyme extraction method [34], and natural deep eutectic solvents combined with ultrasound-assisted enzymolysis method [35]. When selecting a polysaccharide extraction method, various factors such as sample

Table 2
ANOVA for the regression model predicting UICP extraction.

Source	Sum of Squares	df	Mean Square	F-value	P-value	Significance
Model	53.72	14	3.84	243.25	< 0.0001	**
A-Ratio	6.15	1	6.15	389.83	< 0.0001	
B-Tem	4.48	1	4.48	283.86	< 0.0001	
C-Power	5.10	1	5.10	323.08	< 0.0001	
D-Time	4.25	1	4.25	269.33	< 0.0001	
AB	0.3540	1	0.3540	22.44	0.0003	
AC	0.2550	1	0.2550	16.17	0.0013	
AD	0.3660	1	0.3660	23.21	0.0003	
BC	0.1406	1	0.1406	8.92	0.0098	
BD	0.0600	1	0.0600	3.81	0.0714	
CD	0.1369	1	0.1369	8.68	0.0106	
A ²	18.97	1	18.97	1202.94	< 0.0001	
B ²	9.90	1	9.90	627.55	< 0.0001	
C ²	12.20	1	12.20	773.62	< 0.0001	
D ²	8.68	1	8.68	550.09	< 0.0001	
Residual	0.2208	14	0.0158			
Lack of Fit	0.0639	10	0.0064	0.1629	0.9908	Not significant
Pure Error	0.1569	4	0.0392			
Cor Tatal	53.94	28		Predicted R ²	0.9886	
R ²	0.9959	R ² adj	0.9918	C.V.%	0.4840	

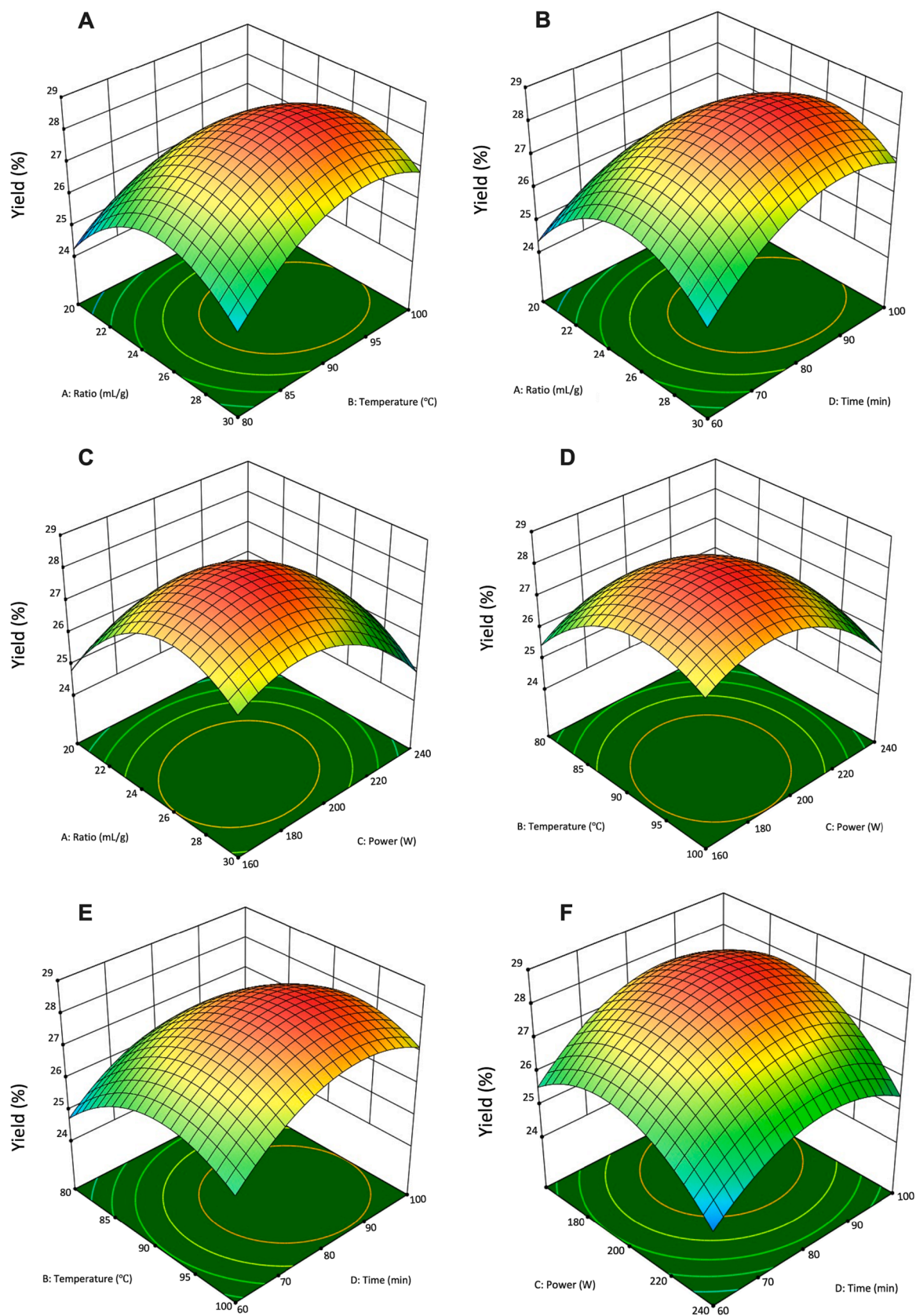


Fig. 2. The 3D surface plots showing interactions of any two variables on ICPs yield.

Table 3
Molecular weight distribution of purified components of polysaccharide.

Samples	Monosaccharide composition	Mn	Mw	PID	Polysaccharide content (%)	Protein content (%)
UICP	Ara, Glc, Gal	51.1 kDa	53.7 kDa	1.05	92.21 ± 0.61	0.17 ± 0.28
ICPC-b	Ara, Glc, Gal	62.3 kDa	69.2 kDa	1.11	85.74 ± 0.28	0.30 ± 0.15

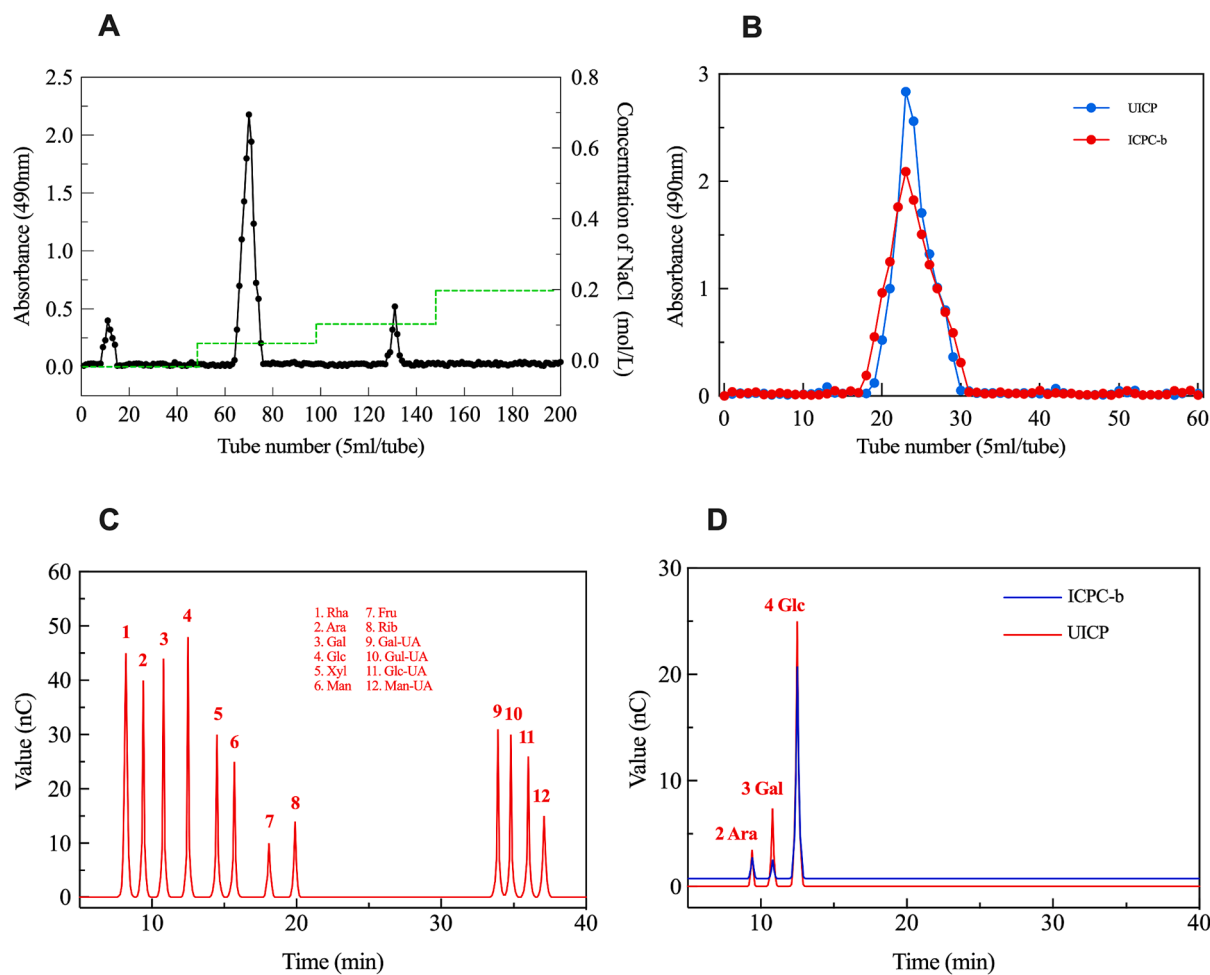


Fig. 3. Purification and monosaccharide composition identification of ICPCs. A, DEAE-52 elution curve; B, Sephadex G-100 elution curve; C, monosaccharide composition standard chromatogram; D, monosaccharide composition analysis of ICPC-b and UICP.

characteristics, extraction efficiency, ease of operation, cost, and environmental impact can be considered.

3.3. Analysis of monosaccharide composition

We obtained purified ICPC-b (hot water) and UICP (ultrasound), and then used HPGPC to detect the molecular weights (Mw) of the two polysaccharides. As shown in the Table 3., ICPC-b and UICP were homogeneous polysaccharides, with Mw values of 62.3 kDa and 51.1 kDa, respectively. The Mw of extracted polysaccharides decreased with increasing ultrasonic intensity is consistent with previous research results [8]. Ultrasonic cavitation can break the glycosidic bonds of polysaccharides, resulting in the production of more low-Mw polysaccharides. Monosaccharide composition results indicated that both ICPC-b and UICP were composed of Ara, Glc, and Gal. UICP had a higher proportion of Ara and Glc (Fig. 3D), which may be attributed to differences in temperature, and extraction mode between different extraction methods, leading to variations in dissolved polysaccharide components. Although the differences in monosaccharide composition

types are small, the variations in content could impact the physicochemical properties of the two polysaccharides, potentially influencing their biological activities [36]. In Wei's previous study, monosaccharide composition types did not change under ultrasonic action, but there were differences in the proportions of each monosaccharide component [18].

3.4. Structural analysis

The infrared absorption spectra of ICPC-b and UICP were shown in the Fig. 4A. In the characteristic frequency region of the infrared spectrum, absorption peaks at 3395.1 cm^{-1} , 2918.2 cm^{-1} , 1635.3 cm^{-1} , 1343.6 cm^{-1} , 3407.4 cm^{-1} , 2923.8 cm^{-1} , 1647.8 cm^{-1} , 1339.3 cm^{-1} were visible, respectively. These peaks were generated by the stretching and vibration of functional groups [37]. In the fingerprint region, prominent absorption peaks were observed at 1268.9 cm^{-1} , 1140.2 cm^{-1} , 1002.7 cm^{-1} , 899.8 cm^{-1} , 831.7 cm^{-1} , 1278.6 cm^{-1} , 1111.7 cm^{-1} , 1006.5 cm^{-1} , 912.1 cm^{-1} , 838.8 cm^{-1} . The multiple peaks were generated by the stretching vibration of single bonds [38]. The

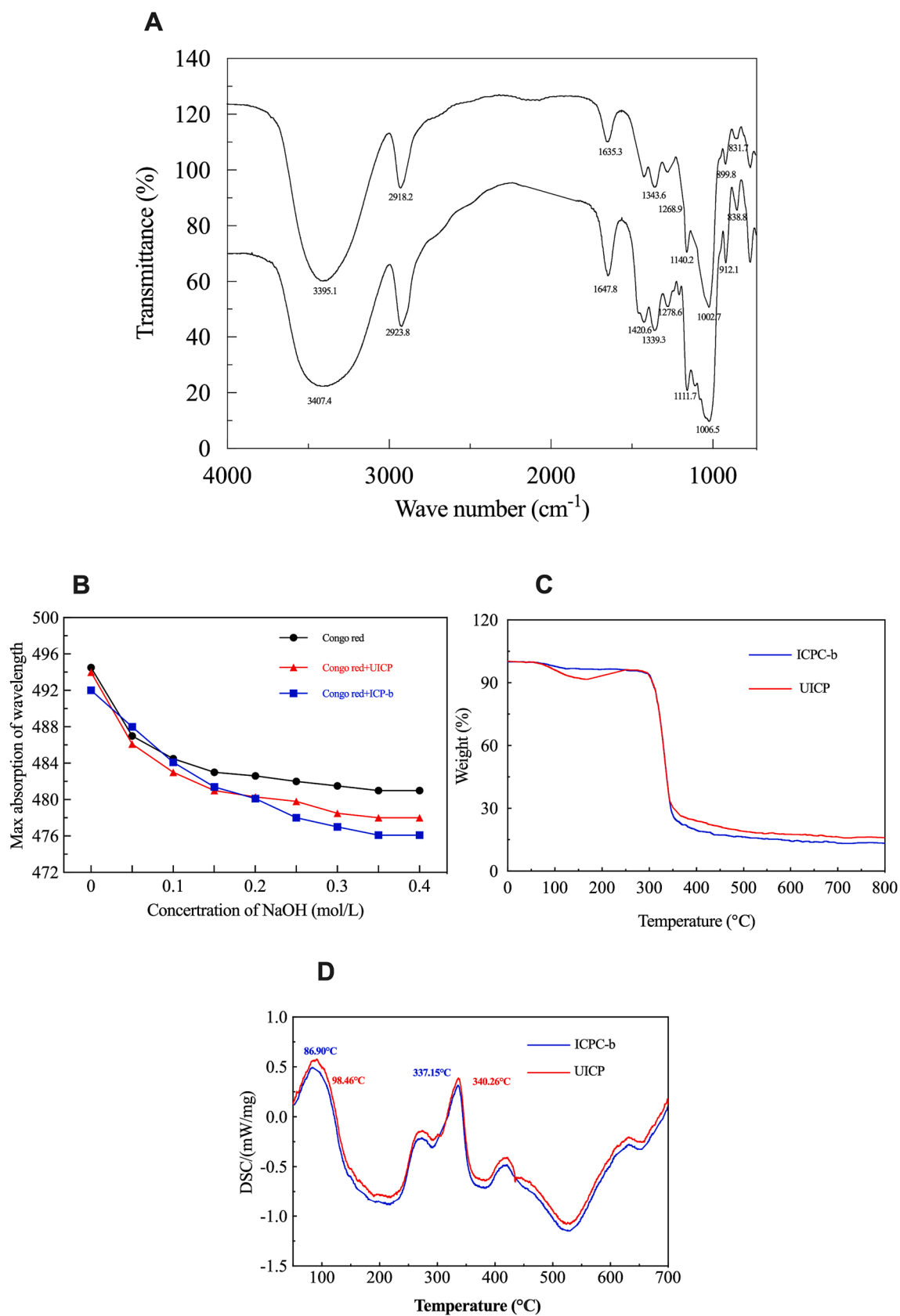


Fig. 4. Structural characteristics and thermal stability of ICPCs. A, Infrared spectrum of ICPCs; B, Congo red analysis; C, TGA analysis; D, DSC thermogram.

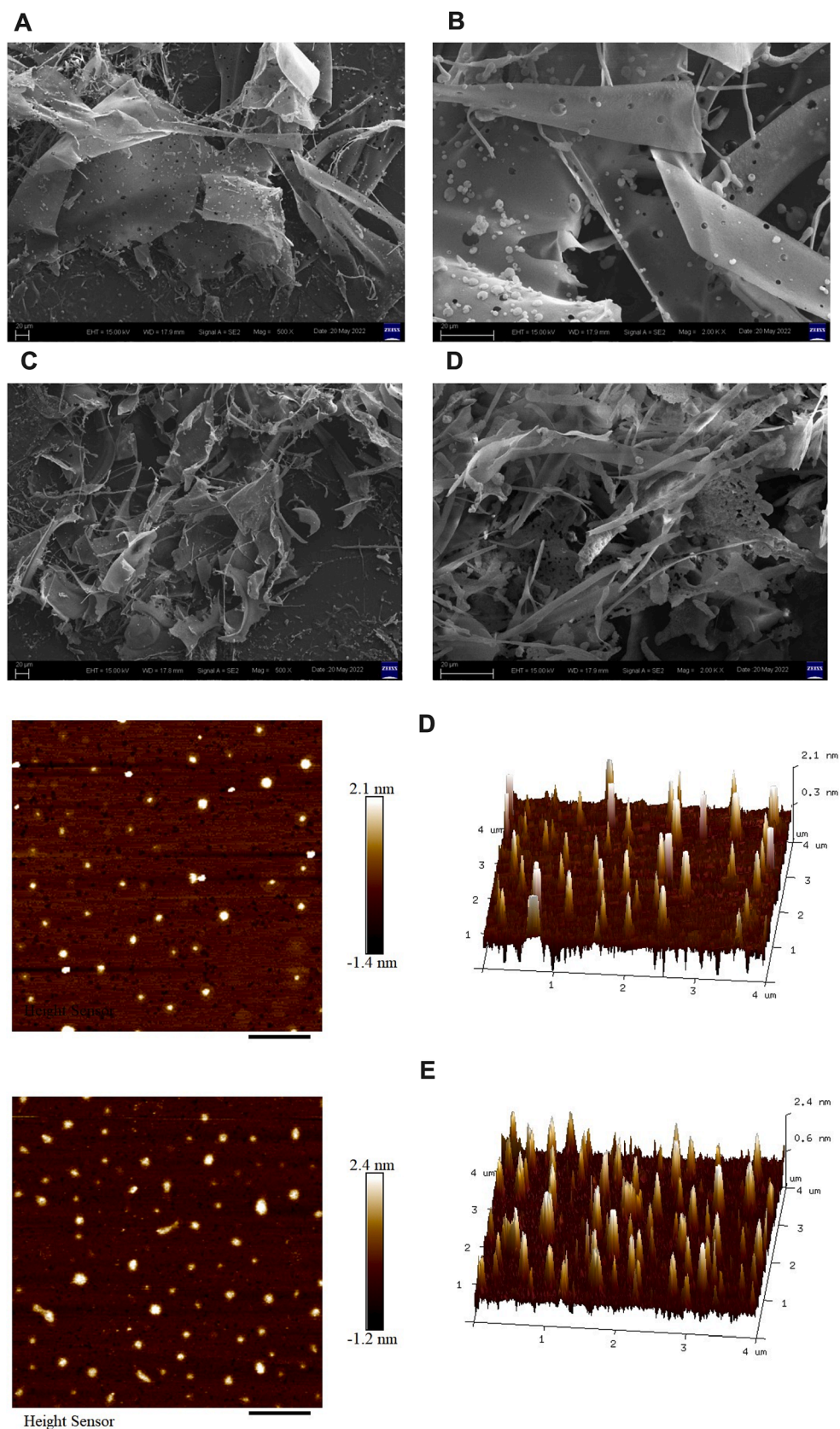


Fig. 5. The SEM and AFM observations of ICPCs. A, B, ICPC-b SEM (500×, 1000 ×); C, D, UICP SEM (500×, 1000 ×); D, ICPC-b AFM images; E, UICP AFM images.

Table 4

Thermogravimetric mass loss spectrum and DSC thermogram.

Samples	Onset temperature (°C)	Peak temperature (°C)	Residual quality (%)
UICP	20.3–169.04	340.26	15.64
ICPC-b	20.3–156.21	337.15	13.42

characteristic absorption peaks at 3395.1 cm^{-1} and 3407.4 cm^{-1} indicating the presence of intermolecular hydrogen bonds in ICPC-b and UICPC-b [39]. Additionally, due to the sharp peak of the alcohol hydroxyl group's fundamental frequency at 3437 cm^{-1} , the peaks at 3395.1 cm^{-1} and 3407.4 cm^{-1} become broad, which may be indicative of the association between $-\text{OH}$ and $-\text{NH}$, causing the absorption peaks to overlap and broaden [40]. The peaks at $3000\text{--}1000\text{ cm}^{-1}$ may be due to the stretching, deformation and vibration of C-H. 1002.7 cm^{-1} , 1111.7 cm^{-1} , and 1006.5 cm^{-1} represented the fingerprint region of pyranose [41]. The peaks observed at 899.8 cm^{-1} , 831.7 cm^{-1} , 912.1 cm^{-1} , 838.8 cm^{-1} suggested the possible presence of α and β -glycosidic bonds in ICPC-b and UICPC-b. These results indicated that ICPC-b and UICPC-b exhibited similar characteristic peaks, and ultrasonic did not significantly impact the main chemical structure of ICPCs [42]. Yuan et al. reported that no significant differences were observed between the characteristic organic groups of polysaccharides extracted from okra by hot water, pressurized water and microwave-assisted techniques [43]. Alboofetileh et al. also found that the three polysaccharides obtained from the brown alga *Nizamuddinina zardinii* with different extraction solvents had similar FT-IR [44], and our results are in agreement with the above studies.

Congo red results showed that the maximum absorption wavelengths

of UICP and ICPC-a gradually decreased, and the trend was similar to that of the Congo red control. It can be concluded that the triple helix structure does not exist in UICP and ICPC-a. Our results were similar to those of Shen et al. The effect of ultrasonic treatment on the three-dimensional structure of polysaccharides does not arise [45].

3.5. SEM analysis

SEM showed the basic morphology of polysaccharide samples through the interaction between the electron beam and the sample to generate the electronic signal imaging reaction [46]. According to the SEM images, the microscopic morphological characteristics, or changes of polysaccharide, including the length of its molecular shape, stretching state, can be intuitively found. The surfaces of UICP and ICPC-b exhibited significant differences in size and shape. ICPC-b exhibited a pronounced, loose, and porous structure. However, after ultrasonic extraction, the original large sheet-like structure transformed into rough, smaller, and loosely fragmented pieces (Fig. 5A–D). This could be attributed to the severe disruption of the microstructure caused by a significant amount of cavitation activity, turbulent shear, and instantaneous high pressure [47]. The appearance of sparsely cross-linked rod-like structures indicated the disruption of intermolecular cross-linking in UICP. These findings validated that ultrasonic degradation could bring about substantial changes in the surface morphology and spatial conformation of ICPCs. This finding is consistent with the conclusion of Li [47], who observed changes in the morphology of *Platycodon grandiflorum* polysaccharides under ultrasonic treatment.

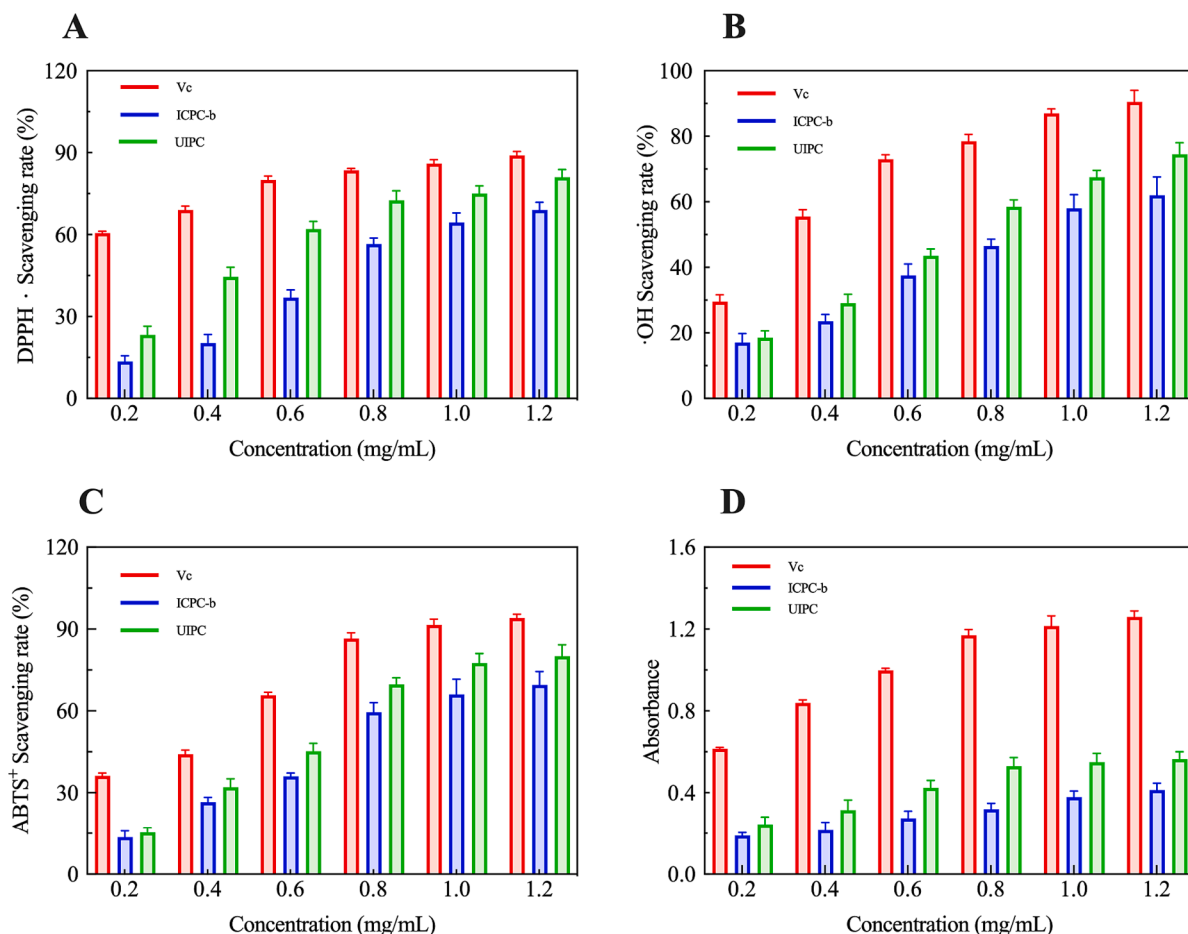


Fig. 6. Analysis of Antioxidant Activity of ICPCs. A, DPPH radical; B, hydroxyl radical; C, ABTS radical; D, reducing power.

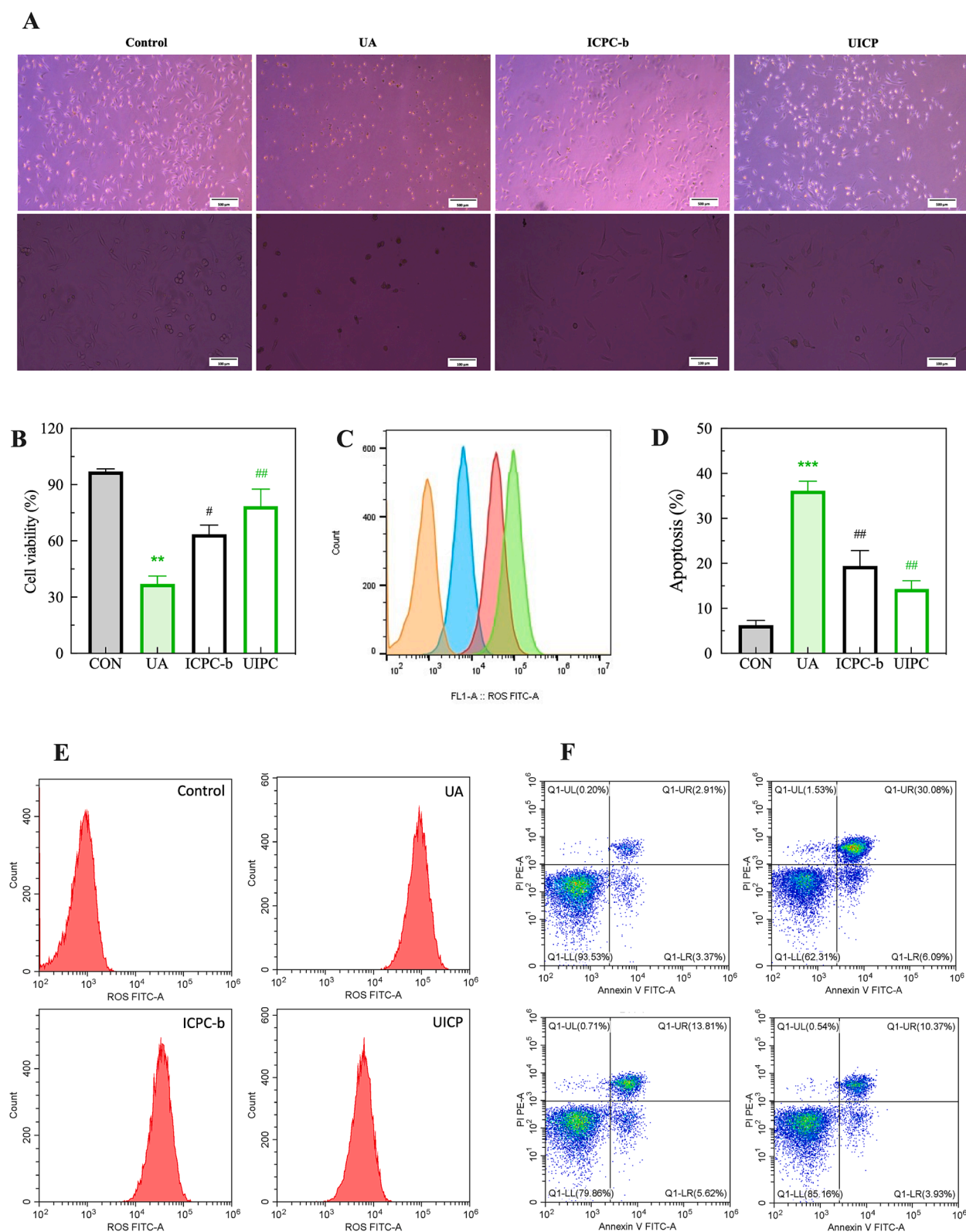


Fig. 7. Effect of ICPs on Uric Acid-Stimulated HK-2 Cells. A, Influence of ICPs on the growth of HK-2 cells stimulated by uric acid; B, CCK-8 cell survival rate; C, E, Flow cytometry detection of ROS levels; D, F, Flow cytometry detection of cell apoptosis levels. #P < 0.05, ##P < 0.01, ###P < 0.001, when compared to the CON group; *P < 0.05, **P < 0.01, ***P < 0.001, when compared to the UA group.

3.6. AFM analysis

AFM is an effective method to directly observe the morphological changes of polysaccharide chains, which can not only observe the

apparent morphology of polysaccharides, but also obtain the morphology of polysaccharides by using the probe to generate relevant signals with the sample surface after reaching a certain distance from the sample surface [48]. The AFM images of UICP and ICPC-b (Fig. 5D and

E) revealed that ICPC-b formed distinct dome-shaped particles, while UICP exhibited irregular ellipsoidal shapes. This suggested that ICs could associate with water in the aqueous environment. The molecular heights of UICP and ICPC-b were 2.4 nm and 2.1 nm, respectively, and the large diameter exceeding 1.0 nm may indicate the entanglement of chains and branches of all polysaccharide components [49]. The degree of polymerization of ICs was moderate, which was conducive to their active function. In addition, similar to the findings of Wang, both UICP and ICPC-b did not exhibit a triple-helix conformation, as their heights were much lower than 15–50 nm [50]. This result is consistent with the results obtained from Congo red testing.

3.7. Thermal stability analysis

Thermal gravimetric (TG) analysis is a thermal analysis method that it can be used to assess information such as the thermal stability and decomposition temperature of the sample [22]. Differential scanning calorimetry (DSC) is commonly employed to measure the rate of heat release or absorption as a function of time or temperature [51]. The TGA curves of ICPC-b and UICP exhibited similar shapes (Fig. 4C) and both showed three distinct mass loss stages. The initial phase (20.3–169.04 °C) was associated with the removal of both bound and free water within the polysaccharide samples, with the temperature turning points for UICP and ICPC-b being 86.90 °C and 98.46 °C, respectively, indicating the glass transition temperature of the polysaccharides. The second stage (300–500 °C) involved the degradation of the polysaccharides themselves. This stage represented the rapid decomposition region for both UICP and ICPC-b, with a loss rate exceeding 50 % of the initial mass. The primary mass loss was attributed to the intense thermal decomposition of polysaccharide molecules, resulting in the release of components such as CO₂ and H₂O [52]. Additionally, in the third stage (500–800 °C), both ICPC-b and UICP exhibited a relatively slow degradation rate, reaching stability at the end. According to the DSC curves, the thermal decomposition temperatures of ICPC-b and UICP throughout the process were 340.26 °C and 337.15 °C, respectively (Fig. 4D, Table 4.). This indicated that ICs possessed good thermal stability, and ultrasound effectively improved the thermal stability of ICs. A similar improvement was found in the thermal stability of *Pueraria Lobata* polysaccharides after ultrasonic degradation [22].

3.8. Analysis of anti-oxidant activity

Most plant polysaccharides have been shown to have anti-oxidant properties [53–55]. In this study, the anti-oxidant activity of ICPC-b and UICP was measured and compared. In this study, the scavenging efficiency and reducing power of UICP on ABTS, DPPH and hydroxyl radical were higher than those of ICPC-b extracted from hot water, with a concentration-dependent behavior. At 1.0 mg/mL, the scavenging rates of DPPH radicals were 69.1 % and 81.2 % for ICPC-b and UICP, respectively (Fig. 6A). The scavenging rates of hydroxyl radicals at 1.0 mg/mL were 62.1 % and 74.5 % for ICPC-b and UICP, respectively (Fig. 6B). The scavenging rates of ABTS radical at 1.0 mg/mL were 69.5 % and 80.3 % for ICPC-b and UICP, respectively (Fig. 6C). In Fig. 6D, the absorbance of UICP treatment was higher than that of ICPC-b, indicating its stronger reducing power. ICPC-b and UICP demonstrated excellent anti-oxidant activity, with UICP exhibiting significantly superior anti-oxidant activity at any concentration. Different structural parameters, such as monosaccharide composition, molecular weight, determine the anti-oxidant properties of ICs. The observed activity is not solely attributed to individual polysaccharide components; instead, it is the synergistic effect of various components [56].

3.9. Cell activity analysis

In the morphology evaluation shown in Fig. 7A, the CON group

exhibited normal overall cell morphology with tightly arranged cells. After uric acid stimulation, the cell counts significantly decreased, cells shrunk, and cell volume reduced. Following intervention with ICPC-b and UICP, cell status tended to normalize, and the cell count significantly increased (Fig. 7B), with UICP mitigating uric acid stimulated cell damage more effectively than ICPC-b. We assessed the impact of ICs on ROS in UA stimulation HK-2 cells using Flow Cytometry. The expression of ROS in cells significantly increased in the UA group. After intervention with ICPC-b and UICP, ROS levels significantly decreased, and UICP had a stronger effect on reducing ROS level (Fig. 7C).

To evaluate the effects of UICP and ICPC-b on UA-stimulated HK-2 cells, cell apoptosis analysis was conducted using Flow Cytometry. After UA stimulation, the percentage of apoptotic cells significantly increased to 36.17 ± 1.57 %. After administration of ICPC-b, the apoptotic cells were significantly lower than in the UA-stimulated, reduced to 19.43 ± 2.43 %, and in the UICP group, it decreased to 14.30 ± 1.30 %. These results suggested that ICs could alleviate UA-induced apoptosis in HK-2 cells, with UICP being more effective than ICPC-b (Fig. 6D).

4. Conclusion

The results indicated that the optimal conditions for polysaccharide extraction were as follows: liquid–solid ratio was 26 mL/g, ultrasound power was 192.75 W, temperature was 90.74 °C, extraction time was 88.84 min, and polysaccharide yield was 28.50 %. Through molecular weight determination, monosaccharide composition analysis, FT-IR spectroscopy, morphology examination, thermal performance assessment, anti-oxidant activity testing, and analysis of the improvement in cell damage caused by uric acid, the impact of different methods on the polysaccharide extraction content was compared. It was found that, ultrasound-assisted provided higher polysaccharide extraction efficiency, lower molecular weight, stronger anti-oxidant activity and ability to ameliorate cellular damage due to uric acid stimulation, and better thermal stability than conventional hot water extraction of polysaccharides.

CRedit authorship contribution statement

Wenchen Yu: Writing – review & editing, Writing – original draft, Supervision, Resources, Project administration, Methodology, Investigation, Formal analysis, Data curation, Conceptualization. **Jiangfei Li:** Conceptualization. **Yi Xiong:** Supervision. **Junwen Wang:** Supervision. **Jiaren Liu:** Formal analysis. **Denis Baranenko:** Visualization. **Yingchun Zhang:** Resources. **Weihong Lu:** Writing – original draft, Funding acquisition.

Declaration of competing interest

The authors declare that they have no known competing financial interests or personal relationships that could have appeared to influence the work reported in this paper.

Acknowledgements

The research was funded by Heilongjiang Touyan Team (HITTY-20190034) and Aerospace Science and Technology Collaborative Innovation Center Project (BSAUEA5740600223)

Thank you, Chen Hui, for your support and encouragement.

References

- [1] Y. Meng, X. Sui, X. Pan, et al., Density-oriented deep eutectic solvent-based system for the selective separation of polysaccharides from *Astragalus membranaceus* var. *mongholicus* under ultrasound-assisted conditions [J], *Ultrason. Sonochem.* 98 (2023) 106522.

- [2] C. Hou, M. Yin, P. Lan, et al., Recent progress in the research of *Angelica sinensis* (Oliv.) diels polysaccharides: extraction, purification, structure and bioactivities [J]. *Chem. Bio. Technol. Agric.* 8 (1) (2021) 13.
- [3] S.-Y. Xu, J.-P. Liu, X. Huang, et al., Ultrasonic-microwave assisted extraction, characterization and biological activity of pectin from jackfruit peel [J], *LWT* 90 (2018) 577–582.
- [4] K. Kumar, S. Srivastav, V.S. Sharanagat, Ultrasound assisted extraction (UAE) of bioactive compounds from fruit and vegetable processing by-products: a review [J], *Ultrason. Sonochem.* 70 (2021) 105325.
- [5] F. Chemat, H. Zill e, M.K. Khan, Applications of ultrasound in food technology: processing, preservation and extraction [J], *Ultrason. Sonochem.* 18 (4) (2011) 813–835.
- [6] R. Cui, F. Zhu, Ultrasound modified polysaccharides: a review of structure, physicochemical properties, biological activities and food applications [J], *Trends Food Sci. Technol.* 107 (2021) 491–508.
- [7] J.S. Zhu, G.M. Halpern, K. Jones, The scientific rediscovery of an ancient chinese herbal medicine: *cordyceps sinensis* part I [J], *J. Altern. Complement. Med.* 4 (3) (1998) 289–303.
- [8] C. Wang, J. Li, Y. Cao, et al., Extraction and characterization of pectic polysaccharides from *Choerospondias axillaris* peels: comparison of hot water and ultrasound-assisted extraction methods [J], *Food Chem.* 401 (2023) 134156.
- [9] L. Martínez Lapuente, Z. Guadalupe, B. Ayestarán, et al., Ultrasound treatment of crushed grapes: effect on the must and red wine polysaccharide composition [J], *Food Chem.* 356 (2021) 129669.
- [10] J. Hu, Y. Liu, L. Cheng, et al., Comparison in bioactivity and characteristics of Ginkgo biloba seed polysaccharides from four extract pathways [J], *Int. J. Biol. Macromol.* 159 (2020) 1156–1164.
- [11] R.-h. Liu, S.-s. Chen, G. Ren, et al., Phenolic compounds from roots of *Imperata cylindrica* var *Major* [J]. *Chinese Herbal Medicines* 5 (3) (2013) 240–243.
- [12] L.-F. Jiang, Cellulase-assisted extraction and antioxidant activity of polysaccharides from rhizoma *imperata* [J], *Carbohydr. Polym.* 108 (2014) 99–102.
- [13] Z.R. Razafindrakoto, N. Tombozara, D. Donno, et al., Antioxidant, analgesic, anti-inflammatory and antipyretic properties, and toxicity studies of the aerial parts of *Imperata cylindrica* (L.) Beauv [J], *S. Afr. J. Bot.* 142 (2021) 222–229.
- [14] J.-Y. Ruan, H.-N. Cao, H.-Y. Jiang, et al., Structural characterization of phenolic constituents from the rhizome of *Imperata cylindrica* var. *major* and their anti-inflammatory activity [J], *Phytochemistry* 196 (2022) 113076.
- [15] X. Li, X. Huang, Y. Feng, et al., Cylindrin from *Imperata cylindrica* inhibits M2 macrophage formation and attenuates renal fibrosis by downregulating the LXR- α /PI3K/AKT pathway [J], *Eur. J. Pharmacol.* 950 (2023) 175771.
- [16] E. Sulistyowati, R.-L. Jan, S.-F. Liou, et al., Vasculoprotective effects of *Centella asiatica*, *justicia gendarussa* and *Imperata cylindrica* decoction via the NOXs-ROS-NF- κ B pathway in spontaneously hypertensive rats [J], *J. Tradit. Complement. Med.* 10 (4) (2020) 378–388.
- [17] Yu W, Xiong Y, Liu M, et al. Structural analysis and attenuates hyperuricemic nephropathy of dextran from the *Imperata cylindrica* Beauv. var. *major* (Nees) C. E. Hubb [J]. *Carbohydrate Polymers*, 2023, 317(12)1064.
- [18] Q. Wei, Y.-h. Zhang, Ultrasound-assisted polysaccharide extraction from *Cercis chinensis* and properties, antioxidant activity of polysaccharide [J], *Ultrason. Sonochem.* 96 (2023) 106422.
- [19] A. Chen, Y. Liu, T. Zhang, et al., Chain conformation, mucoadhesive properties of fucoidan in the gastrointestinal tract and its effects on the gut microbiota [J], *Carbohydr. Polym.* 304 (2023) 120460.
- [20] L. Xu, F. Yang, J. Wang, et al., Anti-diabetic effect mediated by ramulus *mori* polysaccharides [J], *Carbohydr. Polym.* 117 (2015) 63–69.
- [21] D. Ren, Y. Zhao, Y. Nie, et al., Hypoglycemic and hepatoprotective effects of polysaccharides from *Artemisia sphaerocephala* krasch seeds [J], *Int. J. Biol. Macromol.* 69 (2014) 296–306.
- [22] Z. Dou, Y. Zhang, W. Tang, et al., Ultrasonic effects on the degradation kinetics, structural characteristics and protective effects on hepatocyte lipotoxicity induced by palmitic acid of *pueraria lobata* polysaccharides [J], *Ultrason. Sonochem.* 101 (2023) 106652.
- [23] Z. Zhang, F. Kong, H. Ni, et al., Structural characterization, α -glucosidase inhibitory and DPPH scavenging activities of polysaccharides from guava [J], *Carbohydr. Polym.* 144 (2016) 106–114.
- [24] Y. Liu, X. Li, H. Qin, et al., Obtaining non-digestible polysaccharides from distillers' grains of chinese baijiu after extrusion with enhanced antioxidant capability [J], *Int. J. Biol. Macromol.* 243 (2023) 124799.
- [25] Z. Ding, M. Zhao, X. Li, et al., A novel polysaccharide from the fruits of *Cudrania tricuspidata* and its antioxidant and alcohol dehydrogenase activating ability [J], *J. Funct. Foods* 110 (2023) 105850.
- [26] A.D. Premarathna, T.A.E. Ahmed, G. Kulshreshtha, et al., Polysaccharides from red seaweeds: effect of extraction methods on physicochemical characteristics and antioxidant activities [J], *Food Hydrocoll.* 165 (2024) 109307.
- [27] H. Yang, J. Bai, C. Ma, et al., Degradation models, structure, rheological properties and protective effects on erythrocyte hemolysis of the polysaccharides from *Ribes nigrum* L [J], *Int. J. Biol. Macromol.* 165 (2020) 738–746.
- [28] Tao Y, Sun D W. Enhancement of Food Processes by Ultrasound: A Review [J]. *Critical Reviews in Food Science and Nutrition*.
- [29] Q.-A. Zhang, H. Shen, X.-H. Fan, et al., Changes of gallic acid mediated by ultrasound in a model extraction solution [J], *Ultrason. Sonochem.* 22 (2015) 149–154.
- [30] M. Ashokkumar, J. Lee, S. Kentish, et al., Bubbles in an acoustic field: an overview [J], *Ultrason. Sonochem.* 14 (4) (2007) 470–475.
- [31] J. Tan, P. Li, W. Wang, et al., Separation of gallic acid from *Cornus officinalis* and its interactions with corn starch [J], *Int. J. Biol. Macromol.* 208 (2022) 390–399.
- [32] S. Lin, X. Meng, C. Tan, et al., Composition and antioxidant activity of anthocyanins from *Aronia melanocarpa* extracted using an ultrasonic-microwave-assisted natural deep eutectic solvent extraction method [J], *Ultrason. Sonochem.* 89 (2022) 106102.
- [33] W. Xiu, X. Wang, Z. Na, et al., Ultrasound-assisted hydrogen peroxide–ascorbic acid method to degrade sweet corn cob polysaccharides can help treat type 2 diabetes via multiple pathways in vivo [J], *Ultrason. Sonochem.* 101 (2023) 106683.
- [34] B. Lin, S. Wang, A. Zhou, et al., Ultrasound-assisted enzyme extraction and properties of shatian pomelo peel polysaccharide [J], *Ultrason. Sonochem.* 98 (2023) 106507.
- [35] N. Wang, Q. Li, Study on extraction and antioxidant activity of polysaccharides from *radix bupleuri* by natural deep eutectic solvents combined with ultrasound-assisted enzymolysis [J], *Sustain. Chem. Pharm.* 30 (2022) 100877.
- [36] S.M.T. Gharibzadeh, F.J. Marti-Quijal, F.J. Barba, et al., Current emerging trends in antitumor activities of polysaccharides extracted by microwave- and ultrasound-assisted methods [J], *Int. J. Biol. Macromol.* 202 (2022) 494–507.
- [37] D.-T. Wu, Y. He, M.-X. Fu, et al., Structural characteristics and biological activities of a pectic-polysaccharide from okra affected by ultrasound assisted metal-free Fenton reaction [J], *Food Hydrocoll.* 122 (2022) 107085.
- [38] Y. Zhang, L. He, Q. Li, et al., Optimization of ultrasonic-assisted deep eutectic solvent for the extraction of polysaccharides from *Indocalamus tessellatus* leaves and their biological studies [J], *Sustain. Chem. Pharm.* 30 (2022) 100855.
- [39] J. Wang, Z. Li, X. Yang, et al., The antitumor role of a newly discovered α -D-glucan from *holtrichia diomphalia* bates as a selective blocker of aldolase A [J], *Carbohydr. Polym.* 255 (2021) 117532.
- [40] Y. Lin, J. Pi, P. Jin, et al., Enzyme and microwave co-assisted extraction, structural characterization and antioxidant activity of polysaccharides from purple-heart radish [J], *Food Chem.* 372 (2022) 131274.
- [41] D.-T. Wu, Y.-X. Zhao, Q. Yuan, et al., Influence of ultrasound assisted metal-free Fenton reaction on the structural characteristic and immunostimulatory activity of a β -D-glucan isolated from *dictyophora indusiata* [J], *Int. J. Biol. Macromol.* 220 (2022) 97–108.
- [42] Y.S. Jing, L.J. Huang, W.J. Lv, et al., Structural characterization of a novel polysaccharide from pulp tissues of *Litchi chinensis* and its immunomodulatory activity [J], *J. Agric. Food Chem.* 62 (4) (2014) 902–911.
- [43] Q. Yuan, S. Lin, Y. Fu, et al., Effects of extraction methods on the physicochemical characteristics and biological activities of polysaccharides from okra (*Abelmoschus esculentus*) [J], *Int. J. Biol. Macromol.* 127 (2019) 178–186.
- [44] M. Alboofetileh, M. Rezaei, M. Tabarsa, et al., Effect of different non-conventional extraction methods on the antibacterial and antiviral activity of fucoidans extracted from *nizamuddiniah zanardinii* [J], *Int. J. Biol. Macromol.* 124 (2019) 131–137.
- [45] S.-g. Shen, S.-r. Jia, Y.-k. Wu, et al., Effect of culture conditions on the physicochemical properties and antioxidant activities of polysaccharides from *Nostoc flagelliforme* [J], *Carbohydr. Polym.* 198 (2018) 426–433.
- [46] W. Cao, J. Wu, X. Zhao, et al., Structural elucidation of an active polysaccharide from *radix puerariae lobatae* and its protection against acute alcoholic liver disease [J], *Carbohydr. Polym.* 325 (2024) 121565.
- [47] X. Chen, Z. Wang, J. Kan, Polysaccharides from ginger stems and leaves: effects of dual and triple frequency ultrasound assisted extraction on structural characteristics and biological activities [J]. *food, Bioscience* 42 (2021) 101166.
- [48] J. Zhang, C. Wen, W. Qin, et al., Ultrasonic-enhanced subcritical water extraction of polysaccharides by two steps and its characterization from *lentinus edodes* [J], *Int. J. Biol. Macromol.* 118 (2018) 2269–2277.
- [49] S. Pose, A.R. Kirby, J.A. Mercado, et al., Structural characterization of cell wall pectin fractions in ripe strawberry fruits using AFM [J], *Carbohydr. Polym.* 88 (3) (2012) 882–890.
- [50] K.-p. Wang, J. Wang, Q. Li, et al., Structural differences and conformational characterization of five bioactive polysaccharides from *lentinus edodes* [J], *Food Res. Int.* 62 (2014) 223–232.
- [51] L. Feng, N. Han, Y.-B. Han, et al., Structural analysis of a soluble polysaccharide GSPA-0.3 from the root of *Panax ginseng* C. A. Meyer and its adjuvant activity with mechanism investigation [J], *Carbohydr. Polym.* 326 (2024) 121591.
- [52] W. Wang, X. Ma, P. Jiang, et al., Characterization of pectin from grapefruit peel: a comparison of ultrasound-assisted and conventional heating extractions [J], *Food Hydrocoll.* 61 (2016) 730–739.
- [53] P.A.R. Fernandes, M.A. Coimbra, The antioxidant activity of polysaccharides: a structure-function relationship overview [J], *Carbohydr. Polym.* 314 (2023) 120965.
- [54] L.F. Ballesteros, J.A. Teixeira, S.I. Mussatto, Extraction of polysaccharides by autohydrolysis of spent coffee grounds and evaluation of their antioxidant activity [J], *Carbohydr. Polym.* 157 (2017) 258–266.
- [55] M.M. Ahmad, Recent trends in chemical modification and antioxidant activities of plants-based polysaccharides: a review [J], *Carbohydr. Polym. Technol. Appl.* 2 (2021) 100045.
- [56] Y. Zhang, Y. Liu, Y. Cai, et al., Ultrasonic-assisted extraction brings high-yield polysaccharides from kangxian flowers with cosmetic potential [J], *Ultrason. Sonochem.* 100 (2023) 106626.